Solar-Terrestrial Physics. 2025. Vol. 11. Iss.1. P. 56–62. DOI: 10.12737/stp-111202507.

DOI: 10.12737/stp-111202507

Received August 15, 2024
Accepted December 02, 2024

DIURNAL VARIATIONS IN CHARACTERISTICS OF SPORADIC LAYER E_s OVER IRKUTSK

E.A. Voronova
Institute of Solar-Terrestrial Physics SB RAS, Irkutsk, Russia, voronova_ea@iszf.irk.ru

K.G. Ratovsky
Institute of Solar-Terrestrial Physics SB RAS, Irkutsk, Russia, ratovsky@iszf.irk.ru

Abstract. We have studied the morphological features of semidiurnal variations in the occurrence of the sporadic E_s layer (PE_s) and height of the layer (hE_s), using data from the Irkutsk DPS-4 ionosonde (52.3° N, 104.3° E) for 2003–2021. By averaging over all the years, we calculate diurnal variations in PE_s and hE_s for each month. It is observed that the maximum of occurrence PE_s is achieved when the height hE_s decreases; and there is an asymmetry in the maximum of occurrence PE_s: morning maxima are larger than evening ones. These features are interpreted based on the concept of the optimal height for E_s formation and the role of photoionization in forming the sporadic layer.

Keywords: sporadic layer, diurnal variations, occurrence frequency, height, semidiurnal tides.

INTRODUCTION

The sporadic layer E_s is a thin plasma sheet of metal ions formed at heights of the E layer from 90 to 130 km. Sometimes E_s becomes denser than the regular E layer or the F2 layer. In such cases, the E_s layer significantly affects radio signal propagation and F-region ionograms.

The mechanism of formation of the E_s layer is explained by the wind shear theory: ions converge from above and below due to the drift caused by vertically sheared winds, for example, when the zonal eastward wind is below the westward wind. Since ion-neutral collision forces counteract convergence, long-lived metal ions of meteoric origin accumulate in narrow dense plasma sheets that appear mainly in the wind shear convergence zone.

The wind shears necessary for the formation of ionospheric layers at midlatitudes are caused by solar synchronous tides, mainly semidiurnal ones [Forbes et al., 1995]. The close relationship between the E_s layer and tidal winds in the lower thermosphere explains the observed semidiurnal nature of formation of the layers and their regular downward movement (see, e.g., [Gershman et al., 1976; Chavdarov et al., 1975; Mathews, 1998; Haldoupis et al., 2006; Arras et al., 2009; Fytterer et al., 2013; Oikonomou et al., 2014; Pignalberi et al., 2014]). Descending of the layer results from continuous layer reformation: E_s follows the ion convergence node that shifts downward at the phase velocity of the tidal wave. The wind shear theory is confirmed by the correlation between the occurrence of E_s and the horizontal component of the geomagnetic field [Gershman et al., 1976; Haldoupis, 2011].

Sporadic layers are largely formed at high altitudes of the E-region since the vertical convergence of ions occurs there much faster and hence more efficiently. At lower altitudes of the E-region, enhanced ion-neutral collisions reduce the vertical motion of ions, thereby slowing down the accumulation of metal ions. The physical mechanism of layer formation and descending is detailed in the reviews [Gershman et al., 1976; Chavdarov et al., 1975; Haldoupis, 2011].

Diurnal variations in the E_s occurrence rate PE_s for different stations have been studied in numerous papers. Analysis of previous studies has shown that diurnal variations in PE_s can be divided into three types. The first type includes PE_s variations with a dominant semidiurnal component having two pronounced maxima in the morning and evening. The second type contains PE_s variations with an approximately constant level during daylight hours and a decrease at dark time (they differ from the first type in the absence of a well-defined minimum during daylight hours). The third type comprises PE_s variations with a dominant diurnal component having a pronounced maximum at sunlit time.

Variations of the first type are generally observed at midlatitudes in summer. Variations of this type are presented in the data from vertical sounding ionosondes in South Korea at the stations Jeju (33.4° N, 126.3° E) and Icheon (37.1° N, 127.5° E) [Jo et al., 2019]; in Australia and New Zealand at the stations Canberra (35.3° S, 149.0° E), Hobart (42.9° S, 147.3° E), and Christchurch (43.4° S, 172.4° E) [Baggaley, 1989]; in Italy at the stations Gibilmanna (37.9° N, 14.0° E) and Rome (41.8° N, 12.5° E) [Pignalberi et al., 2014]. Arras et al. [2009] have also obtained PE_s variations of the first type, using data from GPS receivers on the CHAMP, GRACE, and FORMOSAT-3/COSMIC satellites, averaged over 50°–55° N; Maeda and Heki [2015], using data from ground-based GPS receivers in central Japan. Note that in [Arras et al., 2009] variations of the first type were recorded in July, April, and January. From April to June and in September–October, PE_s variations of the first type were also observed in ionosonde data from Taiwan (24°58' N, 121°11' E) [Lee et al., 2003].

The PE_s variations of the second type are seen in vertical sounding ionograms in summer at various latitudes, from polar to tropical: on the Antarctic Peninsula (65°15'S, 64°16' W) [Zalizovskiy, 2008]; in Novosibirsk (54.8° N, 82.2° E) [Belinskaya et al. et al., 2022]; in Taiwan

(24°58'N, 121°11'E) [Lee et al., 2003]; on Norfolk Is. (29.0° S, 167.9° E) , and in Townsville (19.6° S, 146.8° E) [Baggaley, 1989]. Interestingly, in the monograph [Chavdarov et al., 1975] variations of the first type are presented as typical diurnal variations of PE$_s$ in summer; whereas in the monograph [Gershman et al., 1976], variations of the second type. When sporadic layers are divided by types [Kokourov et al., 2003], diurnal E$_s$ variations of type C at the sunlit time are variations of the first type, type-F E$_s$ is observed at night; and type-L E$_s$, during morning and evening.

The PE$_s$ variations of the third type can be subdivided into two subtypes. Variations of the first subtype feature maximum PE$_s$ near noon in all months, including the summer period. Such PE$_s$ variations were recorded at the Chinese stations Zhangye (39.2° N, 100.5° E) and Beijing (40.3° N, 116.3° E) [Wang et al., 2022], as well as at the Australian stations Mundaring (32.0° S, 116.2° E) and Brisbane (27.5° S, 152.9° E) [Baggaley, 1989]. In variations of the second subtype, during the transition from summer to winter, the evening maximum of PE$_s$ weakens; and in winter, the only maximum of PE$_s$ is observed in the morning. Similar variations were detected at mid-latitude stations [Baggaley, 1989; Jo et al., 2019; Zalizovsky, 2008; Belinskaya et al., 2022] and at the low-latitude station Taiwan [Lee et al., 2003]. We discuss this transition in more detail later, using Irkutsk ionosonde data as an example.

DATA

We have used data with a time resolution of 15 min for 2003–2021 from the vertical sounding ionosonde DPS-4, installed at a station with coordinates 52.3° N, 104.3° E (Irkutsk). Characteristics of the sporadic layer were taken to be the virtual height hE$_s$, obtained by averaging the values for a given month and local time over 2003–2021, and the occurrence rate PE$_s$, calculated as the ratio of the number of observations of E$_s$ to the total number of measurements for 2003–2021 for a given month and local time. The virtual heights of E$_s$ are close to the true heights for type-F and -L E$_s$, as well as for type-C E$_s$ in cases when the difference between critical frequencies of the sporadic and regular E layers is at least 2 MHz [Chavdarov et al., 1975].

DIURNAL VARIATIONS IN OCCURRENCE RATE AND HEIGHT

Figures 1, 2 illustrate diurnal variations of the occurrence rate PE$_s$ and the height hE$_s$ respectively for all months.

Figures 1, 2 show that the semidiurnal component dominates for hE$_s$ from February to November and for PE$_s$ from April to September and in February. The dominance of the semidiurnal component in diurnal variations of hE$_s$ most likely results from semidiurnal tides in neutral wind variations [Haldoupis, 2011]. Nonetheless, the reason for the dominance of the semidiurnal component in the diurnal variations of PE$_s$ still remains unclear. To identify the relationship between the semidiurnal components of hE$_s$ and PE$_s$, we examine the diurnal variations of hE$_s$ and PE$_s$ in more detail for summer, when the E$_s$ occurrence rate is maximum (Table, Figure 3).

EXPLANATION OF DIURNAL VARIATIONS IN THE OCCURRENCE RATE OF THE SPORADIC LAYER E$_s$ BY OPTIMUM HEIGHT

Figure 3 shows diurnal variations in hE$_s$ and PE$_s$ for June and July. Summer diurnal variations in hE$_s$ and PE$_s$ exhibit the semidiurnal component (morning and evening peaks) and the diurnal one (daytime values exceed nighttime ones). Figure 3 indicates that diurnal PE$_s$ minima are observed during the ascending phases of hE$_s$; and diurnal PE$_s$ maxima, during the descending phases of hE$_s$. The morning and evening peaks of hE$_s$ are close in magnitude, whereas the morning peak of PE$_s$ is higher than the evening peak of PE$_s$. Both the hE$_s$ and PE$_s$ variations have a pronounced semidiurnal component (morning and evening peaks), yet the hE$_s$ and PE$_s$ variations per se do not coincide, demonstrating a delay in PE$_s$ relative to hE$_s$.

Table presents the local time corresponding to sunrise and sunset, the morning and evening peaks of hE$_s$ and PE$_s$, as well as hE$_s$ and PE$_s$ observed when PE$_s$ was maximum. It follows from Table that the morning peaks of the E$_s$ height are observed ~1–1.5 hrs after sunrise, the time spread between different months is 25 min. The morning peaks of the E$_s$ occurrence rate take place ~2–3 hrs after the morning peaks of hE$_s$ (49 min spread), ~4–5 hrs after sunrise (51 min spread).

The evening peaks of hE$_s$ are recorded ~2–3 hrs before sunset (49 min spread). The evening peaks of the E$_s$ occurrence rate are linked to sunset rather than to the evening peaks of hE$_s$. Peaks of PE$_s$ are observed 42–51 min before sunset (9 min spread), whereas the spread relative to the evening peaks of hE$_s$ is 75 min. It can also be noted that the difference between the evening peaks of PE$_s$ and hE$_s$ is ~1 hr less than between the morning peaks of PE$_s$ and hE$_s$. The E$_s$ heights corresponding to the times of maximum PE$_s$ vary from 107 to 110 km in the morning and from 111 to 115 km in the evening.

A similar trend in delays in the peaks of PE$_s$ relative to the peaks of hE$_s$ is valid for most months (Figure 4), where the semidiurnal component of PE$_s$ is quite pronounced (see Figures 1, 2). From February to November, the following sequence takes place: dawn — morning peak of hE$_s$ — morning peak of PE$_s$ — evening peak of hE$_s$ — evening peak of PE$_s$ — sunset, except for January and December.

To explain the regularity of the hE$_s$ and PE$_s$ peaks, we examine the influence of hE$_s$ on E$_s$ forming efficiency [Haldoupis et al., 2023].

1. With increasing height, the recombination rate of metal ions decreases, which contributes to an increase in E$_s$ forming efficiency.

2. As the height increases, the efficiency of collisions and neutrals, which prevent the ions from converging, decreases, which also contributes to an increase in E$_s$ forming efficiency.

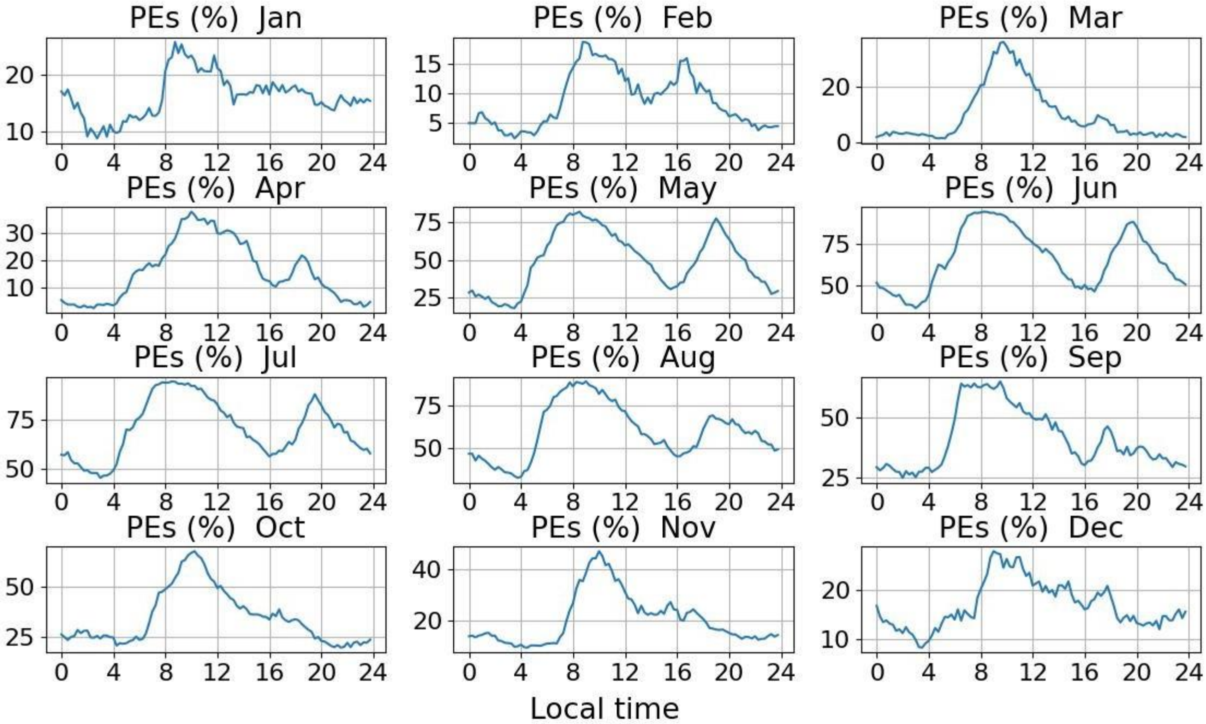

Figure 1. Diurnal variations in the sporadic E-layer occurrence rate PE_s

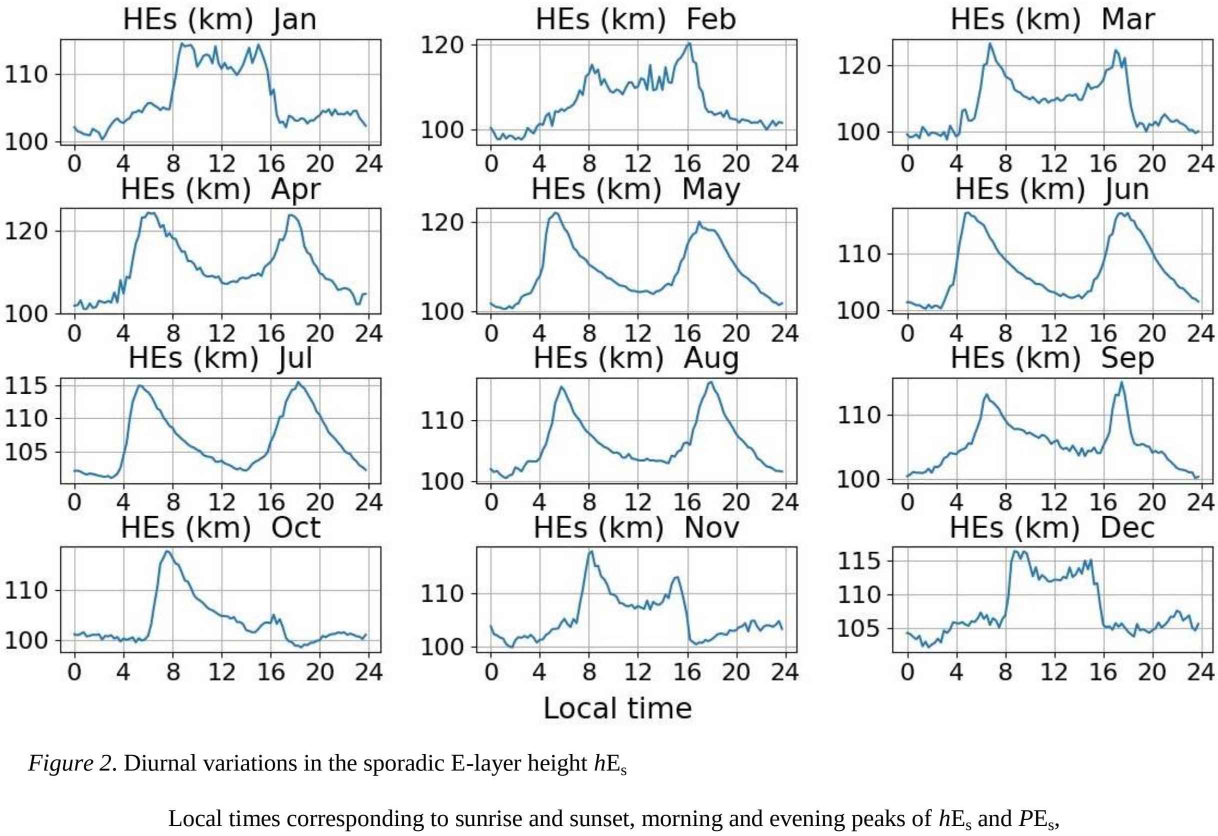

Figure 2. Diurnal variations in the sporadic E-layer height hE_s

Local times corresponding to sunrise and sunset, morning and evening peaks of hE_s and PE_s, as well as hE_s and PE_s observed when PE_s was maximum

Month	Sunrise	LT(hE_s)	LT(PE_s)	hE_s, km	PE_s, %	Sunset	LT(hE_s)	LT(PE_s)	hE_s, km	PE_s, %
May	04:06	05:30	08:30	110	83	19:51	17:00	19:00	115	78
June	03:40	05:00	08:45	107	94	20:26	18:00	19:45	111	89
July	03:59	05:15	08:45	107	95	20:17	18:15	19:30	112	90
August	04:46	05:45	09:00	106	91	19:27	18:00	18:75	113	71

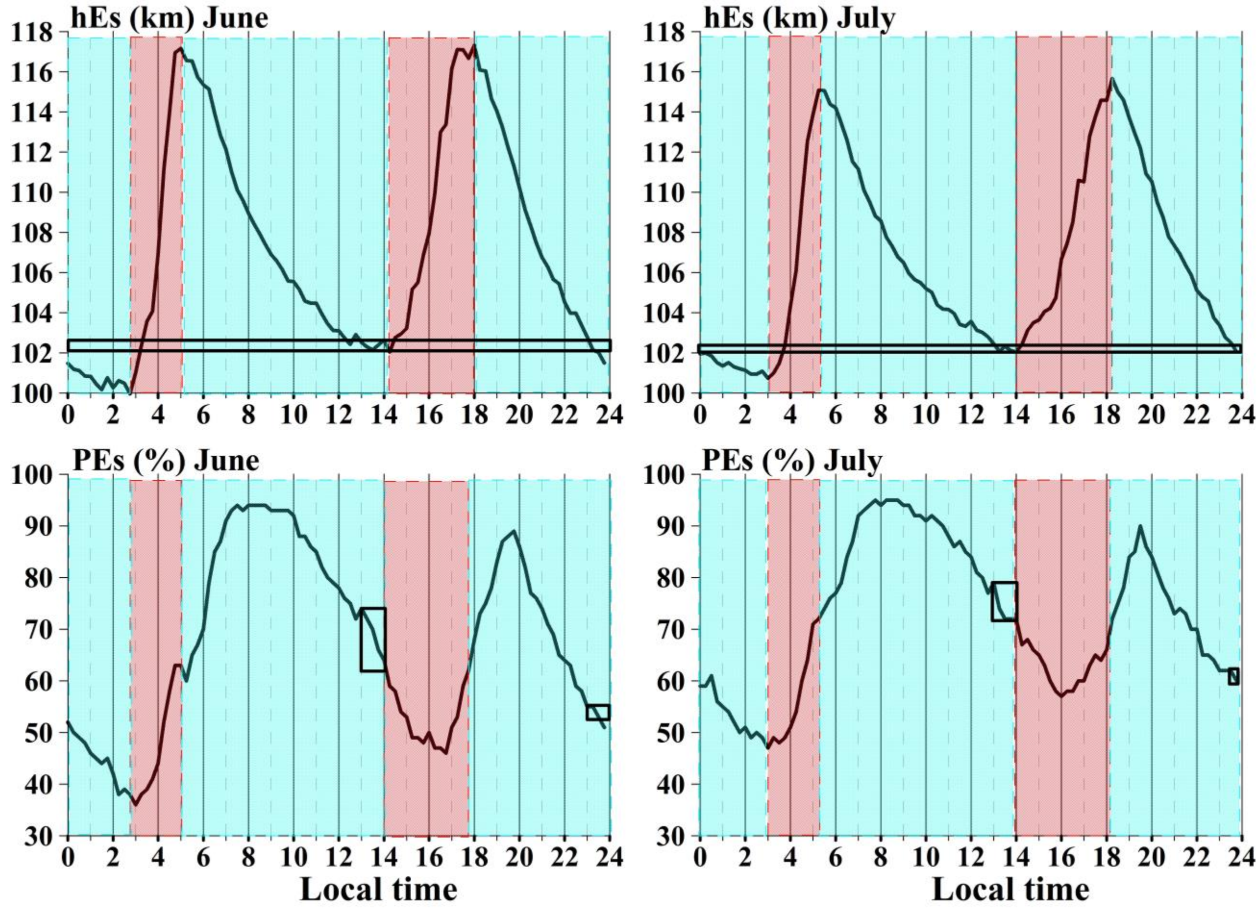

Figure 3. Diurnal variations in hE$_s$ (top) and PE$_s$ (bottom) for June and July; ascending phases of hE$_s$ are highlighted in red; descending phases of hE$_s$, in blue. Rectangles mark the height ranges corresponding to 13:00–14:00 LT (near the diurnal minimum of hE$_s$) (top); the ranges of changes in PE$_s$ corresponding to the intervals when hE$_s$ intersects the height range indicated in top panels (bottom)

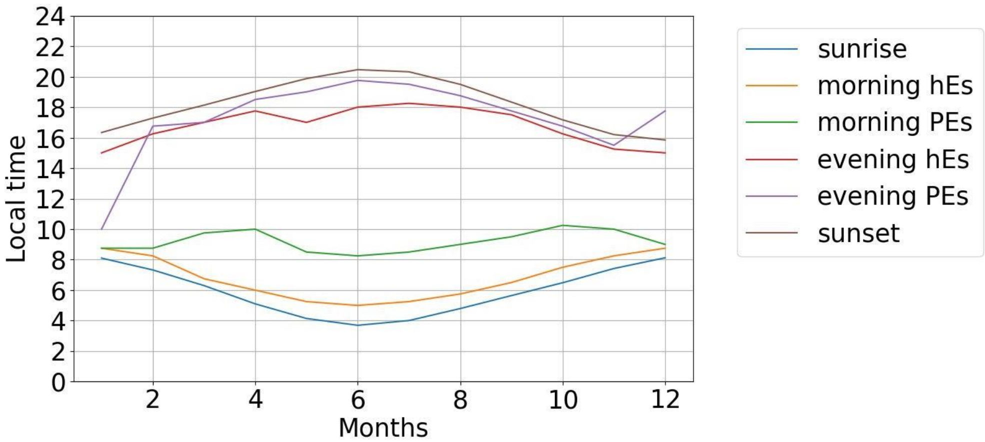

Figure 4. Time of sunrise and sunset, as well as PE$_s$ and hE$_s$ peaks for each month

3. The process of thermal ablation of metal atoms and ions (release due to intense frictional heating) occurs mainly at heights from 80 to 110 km, which contributes to a decrease in E$_s$ forming efficiency with increasing height.

Taking into account all three factors, we can assume that there is an optimum height of E$_s$ formation. Table suggests that this height is between 107 and 110 km in the morning and between 111 and 115 km in the evening.

Existence of the optimum height of E$_s$ formation explains the behavior of PE$_s$ during the descending phase of hE$_s$: first, hE$_s$, decreasing, approaches the optimum height of layer formation and hence PE$_s$ increases; then, continuing to decrease, hE$_s$ moves away from the optimum height and PE$_s$ decreases. Nevertheless, the assumption about the existence of the optimum height does not explain the PE$_s$ minima during the ascending phases of hE$_s$. To clarify this issue, we analyze the diurnal behavior of hE$_s$ in June 2005 without averaging (Figure 5).

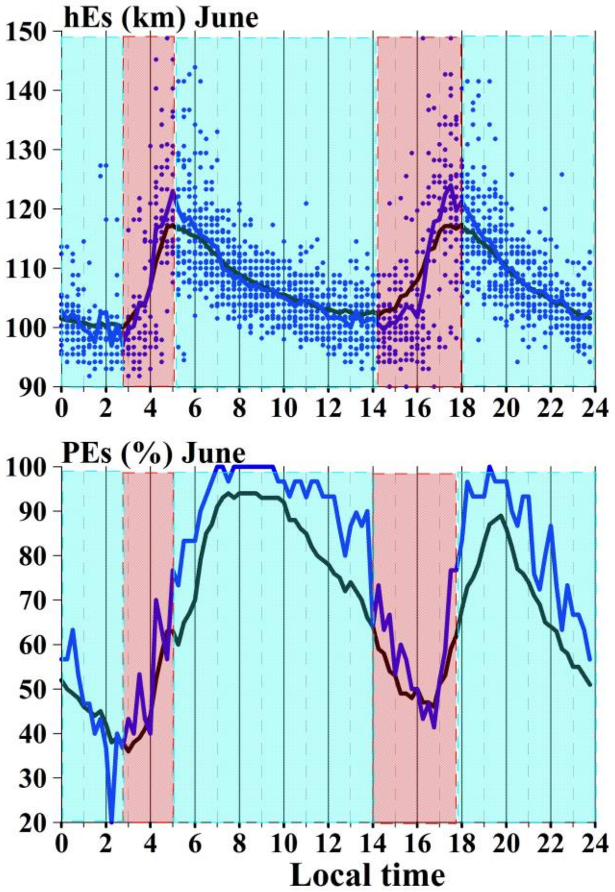

Figure 5. Diurnal behavior of *h*Es (top) and *P*E$_s$ (bottom) in June 2005: blue lines denote averages for all Junes from 2003 to 2021; black lines indicate averages for June 2005; the pink fill marks ascending phases of *h*E$_s$; the blue fill, the descending phase of *h*E$_s$. Blue dots in the top panel show observed values of *h*E$_s$.

In Figure 5, blue dots represent *h*E$_s$ on various days of June 2005 for this local time. Figure 5 demonstrates that during ascending phases of *h*E$_s$ there are reflections as if from the upper and lower sporadic layer (on some days, from the lower layer; on others, from the upper layer). The presence of upper and lower sporadic layers is discussed in more detail below. The increase in the average height of the E$_s$ layer is due to the gradual dominance of reflections from the upper layer. The beginning of the *h*E$_s$ ascending phase approximately coincides with the beginning of reflections from the upper layer; and its end, with the end of reflections from the lower layer. During the ascending phase, reflections generally occur from the layers furthest from the optimum height (both down and up), which explains the *P*E$_s$ minima during the *h*E$_s$ ascending phases.

The presence of upper and lower sporadic layers is illustrated in Figures 6 and 7, which plot the occurrence rate of E$_s$ as a function of height and local time for all Junes and Julies from 2003 to 2021. During the ascending phase of the averaged height when a *P*E$_s$ minimum is observed, E$_s$ layers are mainly recorded in either 95–105 km or 115–125 km. During the descending phase of the averaged height and the maximum occurrence rate, E$_s$ layers are recorded in the height range 105–115 km — near the optimum height of Es-layer formation. Note that the observation times of the upper and lower sporadic layers correspond to the observation times of the type-CL sporadic layer, indicating the simultaneous observation of type-C and -L layers [Kokourov et al., 2003].

As a rule, only one layer is observed by the ionosonde (the presence of two layers is a consequence of observations on different days). In rare cases, two layers are simultaneously detected by the ionosonde. At the same time, data from the incoherent scatter radar in Arecibo demonstrates the regular simultaneous presence of at least two sporadic layers [Christakis et al., 2009].

ROLE OF PHOTOIONIZATION

The diurnal component of *P*E$_s$ (daytime values exceed nighttime ones) can be explained by the diurnal component of *h*E$_s$ (daytime values exceed nighttime ones), but, in our opinion, there are factors that need to be explained by photoionization of metal atoms. Figure 3 shows that for approximately the same range of *h*E$_s$ the daytime *P*E$_s$ values are noticeably higher than the nighttime ones. In June, the range of *h*E$_s$ 102–103 km corresponds to 13–14 and 23–23:30 LT, with *P*E$_s$ varying from 72 to 79 % during the daytime and being ~62 % at night. In July, *h*E$_s$~102 km corresponds to 13–14 and 23:30–23:45 LT, with *P*E$_s$ varying from 57 to 60 % during the day and being ~50 % at night. Another factor explained by the photoionization effect is the asymmetry of the morning and evening *P*E$_s$ peaks. The *P*E$_s$ peaks are higher in the morning than in the evening, and the heights corresponding to the *P*E$_s$ peaks are higher in the evening than in the morning (see Table). This asymmetry can be explained by the fact that the morning decrease in *h*E$_s$ occur during an increase in photoionization; and the evening decrease in *h*E$_s$, during a decrease in photoionization.

The semidiurnal component of *h*E$_s$ (morning and evening peaks) is explained by semidiurnal variations in the position of the wind shear convergence node, which are, in turn, caused by the semidiurnal component of the neutral wind. The diurnal component of *h*E$_s$ (daytime values exceed nighttime ones) may be related to the effect of photoionization. Figure 3 indicates that the minimum values of *h*E$_s$ are approximately the same during the day and the night. Higher averages of *h*E$_s$ in the daytime are associated with the occurrence of reflections from the upper layer at *h*E$_s$~102–103 km, whereas at night reflections from the upper layer occur at *h*E$_s$~100 km. This difference may be due to the fact that at night reflections from the upper layer appear only at dawn and at the beginning of the photoionization process. An alternative explanation is that nighttime *h*E$_s$ may be wind shear convergence nodes conditioned by the diurnal component of the neutral wind.

CONCLUSION

Using data from the Irkutsk ionosonde DPS-4 (52.3° N, 104.3° E) for 2003–2021, we have carried out a morphological analysis of the Es-layer height and

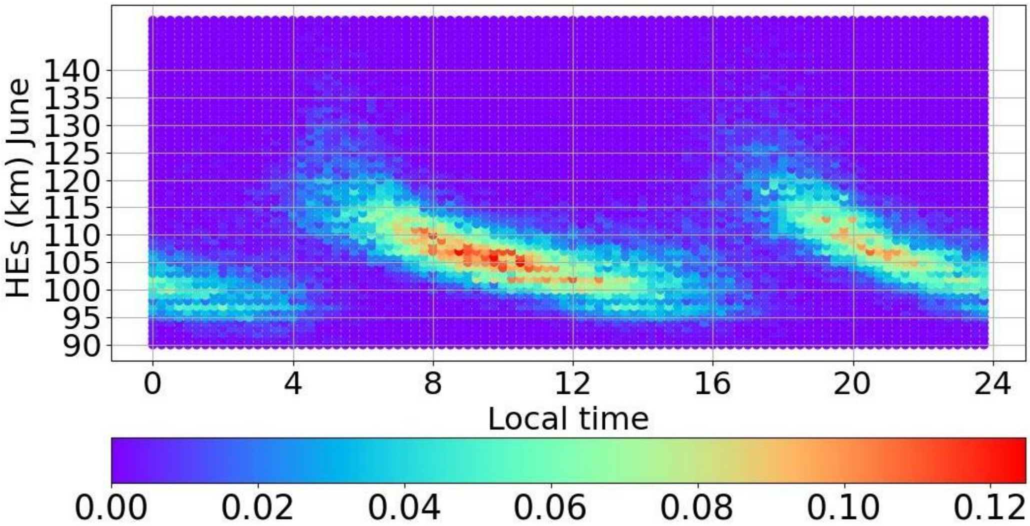

Figure 6. Occurrence rate PE_s as a function of height (with a step of 1 km) and local time (LT=UT+7) for all Junes from 2003 to 2021

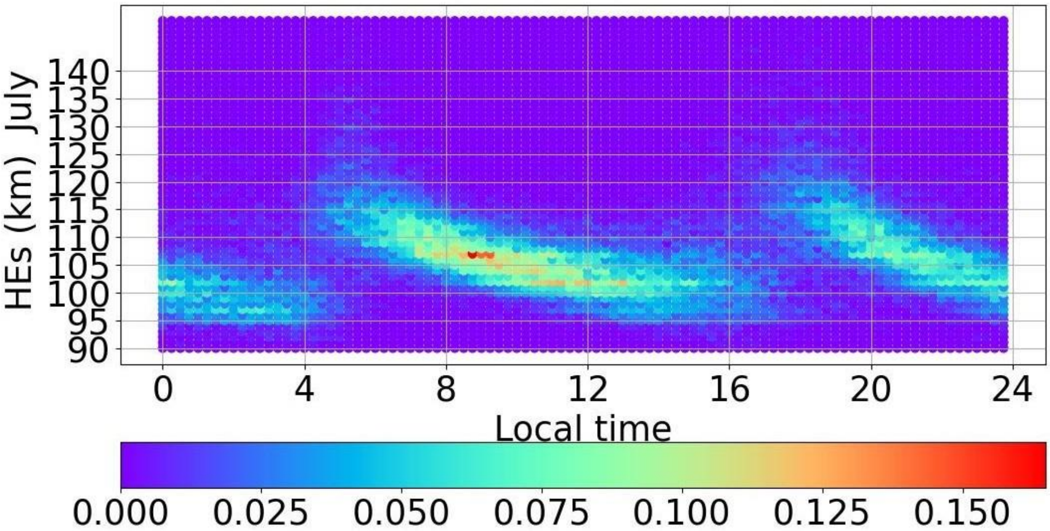

Figure 7. Occurrence rate PE_s as a function of height (with a step of 1 km) and local time (LT=UT+7) for all Julies from 2003 to 2021

occurrence rate. We have found out that the semi diurnal component dominates in both the E_s height and occurrence rate. The dominance of the semidiurnal component in diurnal variations of hE_s stems from semidiurnal tides in the neutral wind [Haldoupis, 2011].

To interpret the dominance of the semidiurnal component in diurnal variations of the E_s occurrence rate, we have proposed a concept of optimum height of sporadic layer formation. Maximum PE_s is observed during the hE_s descending phase when hE_s corresponds to the optimum height of sporadic layer formation. During the ascending phase of the averaged E_s height, reflections generally occur from the layers furthest from the optimum height (both down and up), which explains the E_s occurrence rate minima during the ascending phases of the layer height.

An additional factor influencing diurnal variations in the E_s occurrence rate is photoionization of metal atoms (the probability of E_s formation is proportional to photoionization).

The work was financially supported by the Ministry of Science and Higher Education of the Russian Federation (Subsidy No. 075-GZ/C3569/278). The results were obtained using the equipment of Shared Equipment Center «Angara» [http://ckp-rf.ru/ckp/3056].

REFERENCES

Arras C., Jacobi C., Wickert J. Semidiurnal tidal signature in sporadic E occurrence rates derived from GPS radio occultation measurements at higher midlatitudes. *Ann. Geophys*. 2009, vol. 27, no. 6, pp. 2555–2563. DOI: 10.5194/angeo-27-2555-2009.

Baggaley W.J. Ionospheric E_s in southern hemisphere temperate zone. Seasonal characteristics for f_oE_s, Au_s. *J. Phys*. 1989, vol. 42, no. 4, pp. 451–464. DOI: 10.1071/PH890451.

Belinskaya A.Yu., Kovalev A.A., Karlin V.E. Variations of the E_s layer over Novosibirsk in solar cycles 23 and 24. *Dinamicheskie protsessy v geosferakh* [Dynamic processes in the geospheres]. 2022, vol. 14, no. 1, pp. 93–100. (In Russian).

Chavdarov S.S., Chasovitin Yu.K., Chernysheva S.P., Sheftel V.M. *Sredneshirotnyi sporadicheskii sloi E ionosfery* [Mid-latitude sporadic E layer of the ionosphere]. Moscow, Nauka Publ., 1975, 148 p. (In Russian).

Christakis N., Haldoupis C., Zhou Q., Meek C. Seasonal variability and descent of mid-latitude sporadic E layers at Arecibo. *Ann. Geophys.* 2009, vol. 27, iss. 3, pp. 923–931. DOI: 10.5194/angeo-27-923-2009.

Forbes J.M., Makarov N.A., Portnyagin Yu.I. First results from the meteor radar at South Pole: A large 12-hour oscillation with zonal wavenumber one. *Geophys. Res. Lett*. 1995, vol. 22, no. 23, pp. 3247–3250. DOI: 10.1029/95GL03370.

Fytterer T., Arras C., Jacobi C. Terdiurnal signatures in sporadic E layers at midlatitudes. *Adv. Radio Sci.* 2013, vol. 11, pp. 333–339. DOI: 10.5194/ars-11-333-2013.

Gershman B.N., Ignatiev Yu.A., Kamenetskaya G.Kh. *Mekhanizmy obrazovaniya ionosfernogo sporadicheskogo sloya E_s na razlichnykh shirotakh* [Formation mechanisms of ionospheric sporadic E_s layer at different latitudes]. Moscow, Nauka Publ., 1976, 108 p. (In Russian).

Haldoupis C. *A Tutorial Review on Sporadic E Layers. Aeronomy of the Earth's Atmosphere and Ionosphere*. New York, Springer, 2011, pp. 381–389.

Haldoupis C., Meek C., Christakis N., Pancheva D., Bourdillon A. Ionogram height time intensity observations of descending sporadic E layers at mid-latitude. *J. Atmos. Solar-Terr. Phys*. 2006, vol. 68, no. 3-5, pp. 539–557. DOI: 10.1016/j. jastp.2005.03.020.

Haldoupis C., Haralambous H., Meek C., Mathews J.D. Understanding the diurnal cycle of midlatitude sporadic E. The role of metal atoms. *J. Geophys. Res.: Space Phys*. 2023, vol. 128, no. 4, e2023JA031336. DOI: 10.1029/2023JA031336.

Jo E., Kim Y.H., Moon S., Kwak Y.S. Seasonal and local time variations of sporadic E layer over South Korea. *J. Astron. Space Sci*. 2019, vol. 36, no. 2, pp. 61–68.DOI: 10.5140/JASS. 2019.36.2.61.

Kokourov V.D., Petrukhin V.F., Ponomarev E.A., Sutyrin N.A. Climatic features of the ionosphere E region. *Solnechno-zemnaya fizika* [Solar-Terrestrial Physics]. 2003, iss. 3, pp. 24–27. (In Russian).

Lee C.-C., Liu J.-Y., Pan C.-J., Hsu H.-H. The intermediate layers and associated tidal motions observed by a digisonde in the equatorial anomaly region. *Ann. Geophys*. 2003, vol. 21, no. 4, pp. 1039–1045. DOI: 10.5194/angeo-21-1039-2003.

Maeda J., Heki K. Morphology and dynamics of daytime mid-latitude sporadic-E patches revealed by GPS total electron content observations in Japan. *Earth, Planets and Space*. 2015, vol. 67, no. 89. DOI: 10.1186/s40623-015-0257-4.

Mathews J.D. Sporadic E: Current views and recent progress. *J. Atmos. Solar-Terr. Phys*. 1998, vol. 60, no. 4, pp. 413–435. DOI: 10.1016/S1364-6826(97)00043-6.

Oikonomou C., Haralambous H., Haldoupis C., Meek C. Sporadic E tidal variabilities and characteristics observed with the Cyprus digisonde. *J. Atmos. Solar-Terr. Phys*. 2014, vol. 119, pp. 173–183. DOI: 10.1016/j.jastp.2014.07.014.

Pignalberi A., Pezzopane M., Zuccheretti E. Sporadic E layer at mid-latitudes: Average properties and influence of atmospheric tides. *Ann. Geophys*. 2014, vol. 32, no. 11, pp. 1427–1440. DOI: 10.5194/angeo-32-1427-2014.

Wang W., Jiang C., Wei L., Tang Q., Huang W., Shen H., et al. Comparative study of the E_s layer between the plateau and plain regions in China. *Remote Sens*. 2022, vol. 14, no. 12, id. 2871. DOI: 10.3390/rs14122871.

Zalizovski A.V. The role of tropospheric processes in the formation of sporadic layers of the E-region of the ionosphere over the Antarctic Peninsula. *Radiofizika i radioastronomiya* [Radiophysics and radio astronomy]. 2008, vol. 13, no. 1, pp. 26–38. (In Russian).

URL: http://ckp-rf.ru/ckp/3056/ (accessed November 5, 2024).

Original Russian version: Nikitenko S.A., Lebed O.M., Larchenko A.V., Fedorenko Yu.V., published in Solnechno-zemnaya fizika. 2025, vol. 11, no. 1, pp. 63–69. DOI: 10.12737/szf-111202507.

How to cite this article

Voronova E.A., Ratovsky K.G. Diurnal variations in characteristics of sporadic layer E_s over Irkutsk. *Solar-Terrestrial Physics.* 2025, vol. 11, iss. 1, pp. 56–62. DOI: 10.12737/stp-111202507.